

Processed splitting algorithms for rigid-body molecular dynamics simulations

Igor P. Omelyan

*Institute for Condensed Matter Physics, 1 Sviientsitskii Street, UA-79011 Lviv, Ukraine
and Institute for Theoretical Physics, Linz University, A-4040 Linz, Austria*

(Received 12 March 2008; revised manuscript received 15 May 2008; published 5 August 2008)

An approach for integration of motion in many-body systems of interacting polyatomic molecules is proposed. It is based on splitting time propagation of pseudovariables in a modified phase space, while the real translational and orientational coordinates are decoded by processing transformations. This allows one to overcome the barrier on the order of precision of the integration at a given number of force-torque evaluations per time step. Testing in dynamics of water versus previous methods shows that the algorithms obtained significantly improve the accuracy of the simulations without extra computational costs.

DOI: [10.1103/PhysRevE.78.026702](https://doi.org/10.1103/PhysRevE.78.026702)

PACS number(s): 02.60.Cb, 02.70.Ns, 05.10.-a, 45.40.-f

I. INTRODUCTION

Systems of rigid bodies are widely used to model various phenomena on a broad range of length scales, from the microscopic dynamics of molecules in gases and liquids [1,2] and mesoscopic behavior of polymers and other complex collections in chemical and biological physics [3,4] to macroscopic movement of astrophysical objects in celestial mechanics [5,6]. A lot of approaches, including the traditional Runge-Kutta and predictor-corrector schemes [1] as well as more recent splitting techniques [7–12], have been devised over the years to integrate the rigid-body equations of motion.

Now it is well established that the most adequate integration can be done by splitting the time propagator into analytically solvable parts [13–15]. For Hamiltonian systems this provides the preservation of such essential properties as conservation of volume in phase space and time reversibility. As a result, the splitting algorithms exhibit remarkable stability and thus are ideal for long-duration molecular dynamics (MD) simulations. In addition, these algorithms can be symplectic, i.e., can exactly conserve the total energy associated with a nearby Hamiltonian.

The splitting approach however has a limitation on the order K of precision at each given number n of force-torque evaluations per time step. Note that these evaluations present the most time-consuming part of the propagation. For this reason, the rigid-body motion in MD simulations is integrated mainly by the simplest ($K=2$) Verlet-type algorithms [8–12] with $n=1$. The optimized algorithms [13–15] at $n=2$ can outperform Verlet schemes. But such an optimization does not raise the order of precision and for $K=2$ only modest accuracy can be reached. Higher-order ($K=4$) splitting schemes (note that K should be even to ensure time reversibility) can be derived beginning from $n=3$ [14,15]. The increased computational costs at $n=3$ and $K=4$ can be compensated by the increased precision when adding gradientlike terms to the splitting propagator [15].

Meanwhile, it has been found that the order K of precision can be increased by carrying out supplementary (so-called processed) decompositions apart from the basic (kernel) splitting [16]. For $K=4$, each minimal kernel and processor leads to one force and one force-gradient evaluation. This

yields an effective number $n=2(1+\nu)$, where ν is the relative cost spent on the gradient evaluation with respect to that on the force calculation. The number n can be decreased twice to $n=1+\nu$ by constructing cheap approximate processors [17–19]. Taking into account that the evaluation of one force gradient is more expensive at least by a factor of $\nu=2$ than the calculation of one force [13–15] gives that $n\geq 3$. However, the gradient evaluation may present a difficulty for systems with long-range (e.g., Coulomb) interactions, where the factor ν can be too large [15] because of the necessity to calculate a cumbersome tail (Ewald-summed) contributions. Note also that the processed algorithms of Refs. [17,18] were obtained exclusively for pure translational motion and they are not suitable for rigid-body dynamics. The processing methods introduced in Refs. [16,19] for solving ordinary differential equations are more general but need an adaptation to be exploited in the case of rotational motion. In particular, in contrast to free translational dynamics, the propagator of free rotational motion cannot be handled at once and requires additional splitting into analytically integrable parts [15] or involves special functions [20].

Up to now, no processing schemes were designed and applied to MD simulations of interacting rigid bodies. The rotational motion is much more complicated than translational displacements and thus demands a separate investigation. Moreover, a fundamental theoretical problem about the possibility to overcome the barrier $n=3$ for fourth-order integration still remains open. This overcoming is important from the practical point of view as well, because smaller values of n could noticeably speed up the calculations in view of the restricted capabilities of even supercomputers.

In this paper we develop the processing formalism in the explicit presence of translational and orientational degrees of freedom. We show that use of a proper transformation of phase coordinates allows us to lower the fourth-order barrier to the value $n=2$ with no gradient evaluations. It is proven also that in a specific case of quasi-fourth-order integration the number of force-gradient evaluations per step can be reduced to $n=1$.

The paper is organized as follows. The processed algorithms are consistently derived in Sec. II. Their applications to rigid-body MD simulations and comparison with integrators known previously are presented in Sec. III. Concluding remarks are highlighted in Sec. IV.

II. THEORY

Let us consider a classical system of N interacting rigid polyatomic molecules. The dynamical state of such a system in the laboratory frame is determined by the position \mathbf{r}_i of the center of mass m of the i th molecule, its attitude matrix \mathbf{S}_i , as well as the translational \mathbf{p}_i and angular \mathbf{q}_i momenta. The equations of motion can be written in the compact form $d\boldsymbol{\rho}/dt=L\boldsymbol{\rho}(t)$. Here $\boldsymbol{\rho}=\{\mathbf{r}_1, \mathbf{p}_1, \mathbf{S}_1, \mathbf{q}_1; \dots; \mathbf{r}_N, \mathbf{p}_N, \mathbf{S}_N, \mathbf{q}_N\} \equiv \{\mathbf{r}, \mathbf{p}, \mathbf{S}, \mathbf{q}\}$ is the set of phase variables,

$$L = \sum_{i=1}^N \left(\frac{\mathbf{p}_i}{m} \cdot \frac{\partial}{\partial \mathbf{r}_i} + \mathbf{W}(\mathbf{J}^{-1}\mathbf{S}_i\mathbf{q}_i)\mathbf{S}_i \cdot \frac{\partial}{\partial \mathbf{S}_i} + \mathbf{f}_i(\mathbf{r}, \mathbf{S}) \cdot \frac{\partial}{\partial \mathbf{p}_i} + \mathbf{g}_i(\mathbf{r}, \mathbf{S}) \cdot \frac{\partial}{\partial \mathbf{q}_i} \right) \quad (1)$$

denotes the Liouville operator, \mathbf{f}_i and \mathbf{g}_i are the force and torque, respectively, acting on the molecule due to atomic interactions, and

$$\mathbf{W}(\boldsymbol{\Omega}) = \begin{pmatrix} 0 & \Omega_Z & -\Omega_Y \\ -\Omega_Z & 0 & \Omega_X \\ \Omega_Y & -\Omega_X & 0 \end{pmatrix}$$

is the skew-symmetric matrix related to the principal components $(\Omega_X, \Omega_Y, \Omega_Z)$ of the angular velocity $\boldsymbol{\Omega}=\mathbf{J}^{-1}\mathbf{S}\mathbf{q}$ with $\mathbf{J}=\text{diag}(J_X, J_Y, J_Z)$ being the matrix of moments of inertia. If an initial configuration $\boldsymbol{\rho}(0)$ is specified, the unique solution to the equations of motion can formally be cast for any time t as $\boldsymbol{\rho}(t)=[\exp(Lh)]^k\boldsymbol{\rho}(0)$, where $h=t/k$ is the size of the time step and k denotes the total number of steps.

In the standard splitting approach [13–15], the Liouville operator $L=A+B$ is decomposed into its kinetic $A=m^{-1}\mathbf{p} \cdot \partial/\partial \mathbf{r} + \mathbf{W}(\boldsymbol{\Omega})\mathbf{S} \cdot \partial/\partial \mathbf{S}$ and potential $B=\mathbf{f}(\mathbf{r}, \mathbf{S}) \cdot \partial/\partial \mathbf{p} + \mathbf{g}(\mathbf{r}, \mathbf{S}) \cdot \partial/\partial \mathbf{q}$ parts (we will omit the subscript i for the sake of simplicity). Then the one-step time propagator e^{Lh} can be factorized as $e^{(A+B)h+\mathcal{O}(h^{K+1})}=\prod_{\mu=1}^{n+1}e^{Bb_{\mu}h}e^{Aa_{\mu}h}\equiv\Phi_K(h)$, where $n\geq 1$ and $\{a_{\mu}, b_{\mu}\}$ are chosen in such a way as to provide the highest possible order K of precision, and $\mathcal{O}(h^{K+1})$ denotes the local error. For instance, the second-order ($K=2$) Verlet algorithm is obtained at $n=1$ by $e^{(A+B)h+\mathcal{O}(h^3)}=e^{Bh/2}e^{Ah}e^{Bh/2}\equiv\Phi_2(h)$. Note that the decomposition constants a_{μ} and b_{μ} should enter symmetrically into the factorization to ensure its time reversibility. This reduces the total number of independent constants from $2(n+1)$ to $n+1$. In turn the symmetry provides automatic cancellation of all even-order terms in $\mathcal{O}(h^{K+1})$, leading to evenness of K . For even orders $K\geq 2$, the local error function has the form $\mathcal{O}(h^{K+1})=c_1[A, [A, B]]h^3+c_2[B, [A, B]]h^3+\mathcal{O}(h^{K+3})$, where $[,]$ designates the commutator operation and the coefficients c_1 and c_2 depend on $\{a_{\mu}, b_{\mu}\}$. At $K=2$, the two conditions $\sum_{\mu}a_{\mu}=\sum_{\mu}b_{\mu}=1$ should be satisfied to exclude the zeroth-order term from $\mathcal{O}(h^{K+1})$. In order to increase the precision to $K=4$ we should satisfy the two additional conditions $c_1(\{a_{\mu}, b_{\mu}\})=c_2(\{a_{\mu}, b_{\mu}\})=0$. This can be provided by increasing the number $n+1$ of independent constants at least to the number of the order conditions, i.e., to 4. We see thus that fourth-order ($K=4$) schemes can be constructed only beginning from $n=3$ and this number cannot be lowered within the

standard splitting method. At $n=3$, the fourth-order ($K=4$) factorization can be presented as the concatenation $\Phi_4(h)=\Phi_2(\chi h)\Phi_2((1-2\chi)h)\Phi_2(\chi h)+\mathcal{O}(h^5)$ of three Verlet signatures, where $\chi=1/(2-\sqrt{2})$.

For arbitrary times t , the solution to the equations of motion can be evaluated by consecutively applying k times the one-step splitting propagation $\Phi_K(h)$. This yields $\boldsymbol{\rho}(t)=[\Phi_K(h)]^k\boldsymbol{\rho}(0)+\mathcal{O}(h^K)$, where $\mathcal{O}(h^K)\sim k\mathcal{O}(h^{K+1})$ is the global error due to the accumulation of the local one after $k=t/h\gg 1$ steps. The action of the exponential operators $e^{A\tau}$ and $e^{B\tau}$ on a phase space point $\boldsymbol{\rho}$ is given analytically by

$$e^{A\tau}\{\mathbf{r}, \mathbf{p}, \mathbf{S}, \mathbf{q}\} = \{\mathbf{r} + m^{-1}\mathbf{p}\tau, \mathbf{p}, \boldsymbol{\Xi}(\mathbf{q}, \tau)\mathbf{S}, \mathbf{q}\},$$

$$e^{B\tau}\{\mathbf{r}, \mathbf{p}, \mathbf{S}, \mathbf{q}\} = \{\mathbf{r}, \mathbf{p} + \mathbf{f}(\mathbf{r}, \mathbf{S})\tau, \mathbf{S}, \mathbf{q} + \mathbf{g}(\mathbf{r}, \mathbf{S})\tau\}, \quad (2)$$

where the shift of \mathbf{r} corresponds to free translational motion (at constant \mathbf{p}), while the changes in \mathbf{p} and \mathbf{q} relate to motion in instantaneous force-torque fields [15]. The matrix $\boldsymbol{\Xi}(\mathbf{q}, \tau)$ exactly propagates \mathbf{S} over time τ according to the free rotational dynamics (\mathbf{q} remains constant) $d\mathbf{S}/dt=\mathbf{W}(\mathbf{J}^{-1}\mathbf{S}\mathbf{q})\mathbf{S}$. Expressions for $\boldsymbol{\Xi}(\mathbf{q}, \tau)$ in terms of efficient routines for the elliptic and theta functions are reported in Ref. [20]. Alternatively, $\boldsymbol{\Xi}(\mathbf{q}, \tau)$ can be replaced by its second- or fourth-order counterpart $\boldsymbol{\Xi}_2(\tau)=\boldsymbol{\Psi}_X(\frac{\tau}{2})\boldsymbol{\Psi}_Y(\frac{\tau}{2})\boldsymbol{\Psi}_Z(\tau)\boldsymbol{\Psi}_Y(\frac{\tau}{2})\boldsymbol{\Psi}_X(\frac{\tau}{2})$ or $\boldsymbol{\Xi}_4(\tau)=\boldsymbol{\Xi}_2(\chi\tau)\boldsymbol{\Xi}_2((1-2\chi)\tau)\boldsymbol{\Xi}_2(\chi\tau)$, where $\boldsymbol{\Psi}_{\zeta}(\tau)=\exp[\mathbf{W}(\boldsymbol{\Omega}_{\zeta})\tau]\equiv\boldsymbol{\Theta}(\boldsymbol{\Omega}_{\zeta}, \tau)$ is the matrix representing rotation through angle $\boldsymbol{\Omega}_{\zeta}\tau$ around axis ζ at constant component $\boldsymbol{\Omega}_{\zeta}$ of $\boldsymbol{\Omega}=\mathbf{J}^{-1}\mathbf{S}\mathbf{q}$ [see Eq. (19) of Ref. [15] for $\boldsymbol{\Theta}(\boldsymbol{\Omega}_{\zeta}, \tau)$]. Note that each force-torque recalculation in $e^{B\tau}$ requires $\propto N^2$ operations and is the most time-consuming part of the splitting propagation, while the costs for handling $e^{A\tau}$ are negligible (proportional to N) when $N\gg 1$. The total number of force-torque recalculations per step in Φ_K is equal to n .

The commutators $[A, [A, B]]$ and $[B, [A, B]]$ which appear in the local error function $\mathcal{O}(h^{K+1})$ can be calculated explicitly using the expressions for operators A and B . Then, in the case of the Verlet algorithm ($K=2$), we find $c_1=1/12=2c_2$ and $\mathcal{O}(h^3)=-2m^{-1}\dot{\mathbf{f}} \cdot \partial/\partial \mathbf{r}-\dot{\mathbf{f}} \cdot \partial/\partial \mathbf{p}h^3/12+\mathcal{O}(h^5)$, where at the moment the orientational degrees of freedom were frozen to simplify the notation. Transferring now the corresponding parts of $\mathcal{O}(h^3)$ from $e^{Lh+\mathcal{O}(h^3)}$ to the right under the exponentials e^{Ah} and $e^{Bh/2}$, one obtains $e^{Lh}=e^{Bh/2}e^{Ah}e^{Bh/2}+\mathcal{O}(h^5)$, where $A=A+m^{-1}\dot{\mathbf{f}} \cdot \partial/\partial \mathbf{r}h^2/6$ and $B=B-\dot{\mathbf{f}} \cdot \partial/\partial \mathbf{p}h^2/12$ are the modified counterparts of A and B . Thus, the order of the Verlet signature can increase from $K=2$ to 4 when the decomposition is performed for the nearby Liouvillian $\mathcal{L}=A+B=L(1+m^{-1}\dot{\mathbf{f}} \cdot \partial/\partial \mathbf{r}h^2/6-\dot{\mathbf{f}} \cdot \partial/\partial \mathbf{p}h^2/12)$, where the equalities $\dot{\mathbf{f}}=d\mathbf{f}/dt=L\mathbf{f}$ and $\dot{\mathbf{f}}=L\dot{\mathbf{f}}$ for the time derivatives of \mathbf{f} have been applied. Note, however, that the nearby exponentials $e^{A\tau}$ and $e^{B\tau}$ cannot be handled analytically in $\boldsymbol{\rho}$ space [unlike $e^{A\tau}$ and $e^{B\tau}$, see Eq. (2)], because of the existence of complicated functions $\dot{\mathbf{f}}\equiv\dot{\mathbf{f}}(\boldsymbol{\rho})$ and $\ddot{\mathbf{f}}\equiv\ddot{\mathbf{f}}(\boldsymbol{\rho})$ which contrary to the force field $\mathbf{f}(\mathbf{r}, \mathbf{S})$ depend not only on the positions (\mathbf{r}, \mathbf{S}) but on the momenta (\mathbf{p}, \mathbf{q}) as well.

The main idea of our approach consists in finding such a processing transformation $\tilde{\boldsymbol{\rho}}=\mathcal{T}\boldsymbol{\rho}$ from the phase space point $\boldsymbol{\rho}$ to a new set $\tilde{\boldsymbol{\rho}}$ of variables to make the action of the nearby

exponentials analytically calculable. Taking into account the explicit structure for the nearby Liouvillian \mathcal{L} , the general form of the desired transformation reads $\mathcal{T}=(\mathbf{r}+\alpha m^{-1}\mathbf{f}h^2)\partial/\partial\mathbf{r}+(\mathbf{p}+\beta\dot{\mathbf{f}}h^2)\partial/\partial\mathbf{p}+\mathcal{O}(h^4)\equiv\mathcal{T}_{\alpha,\beta}$, where α and β are some coefficients which will be defined below. It can be verified readily that in the new variables the equations of motion become $d\tilde{\boldsymbol{\rho}}/dt=\tilde{\mathcal{L}}\tilde{\boldsymbol{\rho}}$, where $\tilde{\mathcal{L}}=\tilde{\mathcal{A}}+\tilde{\mathcal{B}}$ is the corresponding Liouville operator with $\tilde{\mathcal{A}}=m^{-1}[\tilde{\mathbf{p}}+(\alpha-\beta)\dot{\mathbf{f}}(\tilde{\mathbf{r}})h^2]\cdot\partial/\partial\tilde{\mathbf{r}}$ and $\tilde{\mathcal{B}}=[\mathbf{f}(\tilde{\mathbf{r}}-\alpha m^{-1}\mathbf{f}(\tilde{\mathbf{r}})h^2)+\beta\dot{\mathbf{f}}(\tilde{\mathbf{r}})h^2]\cdot\partial/\partial\tilde{\mathbf{p}}$. Then for the nearby counterparts of $\tilde{\mathcal{A}}$ and $\tilde{\mathcal{B}}$ one finds $\tilde{\mathcal{A}}=\tilde{\mathcal{A}}+m^{-1}\dot{\mathbf{f}}(\tilde{\mathbf{r}})\cdot\partial/\partial\tilde{\mathbf{r}}h^2/6$ and $\tilde{\mathcal{B}}=\tilde{\mathcal{B}}-\dot{\mathbf{f}}(\tilde{\mathbf{r}})\cdot\partial/\partial\tilde{\mathbf{p}}h^2/12$. We see that the terms with $\dot{\mathbf{f}}$ and $\ddot{\mathbf{f}}$ can be removed in $\tilde{\mathcal{A}}$ and $\tilde{\mathcal{B}}$ by putting $(\alpha-\beta)=-1/6$ and $\beta=1/12$, i.e., $\alpha=-1/12$. The orientational degrees of freedom can be included in a similar manner, leading to the total processing transformation

$$\mathcal{T}_{\alpha,\beta}=(\mathbf{r}+\alpha m^{-1}\mathbf{f}h^2)\frac{\partial}{\partial\mathbf{r}}+(\mathbf{p}+\beta\dot{\mathbf{f}}h^2)\frac{\partial}{\partial\mathbf{p}}+\Theta(\mathbf{J}^{-1}\mathbf{S}\mathbf{g}(\mathbf{r},\mathbf{S}),\alpha h^2)\mathbf{S}\frac{\partial}{\partial\mathbf{S}}+(\mathbf{q}+\beta\dot{\mathbf{g}}h^2)\frac{\partial}{\partial\mathbf{q}}+\mathcal{O}(h^4)$$

and the nearby operators $\tilde{\mathcal{A}}=m^{-1}\tilde{\mathbf{p}}\cdot\partial/\partial\tilde{\mathbf{r}}+\mathbf{W}(\mathbf{J}^{-1}\tilde{\mathbf{S}}\tilde{\mathbf{q}})\tilde{\mathbf{S}}\cdot\partial/\partial\tilde{\mathbf{S}}$ and $\tilde{\mathcal{B}}=\mathbf{f}(\tilde{\mathbf{r}}_\gamma,\tilde{\mathbf{S}}_\gamma)\cdot\partial/\partial\tilde{\mathbf{p}}+\mathbf{g}(\tilde{\mathbf{r}}_\gamma,\tilde{\mathbf{S}}_\gamma)\cdot\partial/\partial\tilde{\mathbf{q}}\equiv\tilde{\mathcal{B}}_\gamma$ at $\alpha=-1/12$, $\beta=1/12$, and $\gamma=-\alpha=1/12$. Here $\Theta(\mathbf{J}^{-1}\mathbf{S}\mathbf{g}(\mathbf{r},\mathbf{S}),\alpha h^2)=\exp[\mathbf{W}(\mathbf{Q})\alpha h^2]$ is the matrix representing three-dimensional rotation, i.e., $\Theta(\mathbf{Q},\tau)=\mathbf{I}\cos(Q\tau)+[1-\cos(Q\tau)][\mathbf{W}(\mathbf{Q})\mathbf{W}(\mathbf{Q})/Q^2+\mathbf{I}]+\sin(Q\tau)\mathbf{W}(\mathbf{Q})/Q$ with \mathbf{I} being the unit matrix, around vector $\mathbf{Q}=\mathbf{J}^{-1}\mathbf{S}\mathbf{g}$ at the angle $Q\alpha h^2$, and $\{\tilde{\mathbf{r}}_\gamma,\tilde{\mathbf{S}}_\gamma\}=\mathcal{T}_{\gamma,0}\{\tilde{\mathbf{r}},\tilde{\mathbf{S}}\}$ is the auxiliary position and attitude matrix.

From the aforesaid, we have for the one-step propagation in $\tilde{\boldsymbol{\rho}}$ space that $\tilde{\boldsymbol{\rho}}(t+h)=e^{\tilde{\mathcal{L}}h}\tilde{\boldsymbol{\rho}}(t)=e^{\tilde{\mathcal{B}}_\gamma h/2}e^{\tilde{\mathcal{A}}h}e^{\tilde{\mathcal{B}}_\gamma h/2}\tilde{\boldsymbol{\rho}}(t)+\mathcal{O}(h^5)$. In $\boldsymbol{\rho}$ space the solution can be reproduced by applying the inverse transformation $\mathcal{T}_{\alpha,\beta}^{-1}$ as $\boldsymbol{\rho}(t+h)=e^{Lh}\boldsymbol{\rho}(t)=\mathcal{T}_{\alpha,\beta}^{-1}\tilde{\boldsymbol{\rho}}(t+h)$. This leads to the resulting propagation of $\boldsymbol{\rho}$ in the form

$$e^{Lh}=\mathcal{T}_{\alpha,\beta}^{-1}e^{\tilde{\mathcal{B}}_\gamma h/2}e^{\tilde{\mathcal{A}}h}e^{\tilde{\mathcal{B}}_\gamma h/2}\mathcal{T}_{\alpha,\beta}+\mathcal{O}(h^5), \quad (3)$$

where $\alpha=-1/12$, $\beta=1/12$, and $\gamma=1/12$. The operator $\mathcal{T}_{\alpha,\beta}$ transforms a phase space point $\boldsymbol{\rho}$ to the set $\tilde{\boldsymbol{\rho}}=\mathcal{T}_{\alpha,\beta}\boldsymbol{\rho}\equiv\{\tilde{\mathbf{r}},\tilde{\mathbf{p}},\tilde{\mathbf{S}},\tilde{\mathbf{q}}\}$ of time-step-dependent pseudovariables, where

$$\begin{aligned} \tilde{\mathbf{r}} &= \mathbf{r} + \alpha m^{-1}\mathbf{f}(\mathbf{r},\mathbf{S})h^2, & \tilde{\mathbf{p}} &= \mathbf{p} + \beta\dot{\mathbf{f}}(\boldsymbol{\rho})h^2, \\ \tilde{\mathbf{S}} &= \Theta(\mathbf{J}^{-1}\mathbf{S}\mathbf{g}(\mathbf{r},\mathbf{S}),\alpha h^2)\mathbf{S}, & \tilde{\mathbf{q}} &= \mathbf{q} + \beta\dot{\mathbf{g}}(\boldsymbol{\rho})h^2. \end{aligned} \quad (4)$$

The action of the exponential operators $e^{\tilde{\mathcal{A}}\tau}$ and $e^{\tilde{\mathcal{B}}_\gamma\tau}$ can be given analytically as

$$\begin{aligned} e^{\tilde{\mathcal{A}}\tau}\tilde{\boldsymbol{\rho}} &= \{\tilde{\mathbf{r}} + m^{-1}\tilde{\mathbf{p}}\tau, \tilde{\mathbf{p}}, \tilde{\mathbf{S}}, \tilde{\mathbf{q}}\}, \\ e^{\tilde{\mathcal{B}}_\gamma\tau}\tilde{\boldsymbol{\rho}} &= \{\tilde{\mathbf{r}}, \tilde{\mathbf{p}} + \mathbf{f}(\tilde{\mathbf{r}}_\gamma,\tilde{\mathbf{S}}_\gamma)\tau, \tilde{\mathbf{S}}, \tilde{\mathbf{q}} + \mathbf{g}(\tilde{\mathbf{r}}_\gamma,\tilde{\mathbf{S}}_\gamma)\tau\}. \end{aligned} \quad (5)$$

Expressions (5) are similar to Eq. (2), since besides the formal replacement of $\boldsymbol{\rho}$ by $\tilde{\boldsymbol{\rho}}$ the only difference between (A,B) and $(\tilde{\mathcal{A}},\tilde{\mathcal{B}})$ lies in the modification of the force

$\mathbf{f}(\tilde{\mathbf{r}}_\gamma,\tilde{\mathbf{S}}_\gamma)$ and torque $\mathbf{g}(\tilde{\mathbf{r}}_\gamma,\tilde{\mathbf{S}}_\gamma)$. Apart from the calculation of their basic values $\mathbf{f}(\tilde{\mathbf{r}},\tilde{\mathbf{S}})$ and $\mathbf{g}(\tilde{\mathbf{r}},\tilde{\mathbf{S}})$, the modification requires (for $\gamma\neq 0$) one extra force-torque evaluation at the auxiliary positional $\tilde{\mathbf{r}}_\gamma=\tilde{\mathbf{r}}+\gamma m^{-1}\mathbf{f}(\tilde{\mathbf{r}},\tilde{\mathbf{S}})h^2$ and orientational $\tilde{\mathbf{S}}_\gamma=\Theta(\mathbf{J}^{-1}\tilde{\mathbf{S}}\mathbf{g}(\tilde{\mathbf{r}},\tilde{\mathbf{S}}),\gamma h^2)\tilde{\mathbf{S}}$ coordinates. This increases the number of force-torque calculations in $e^{\tilde{\mathcal{B}}_\gamma\tau}$ from $n=1$ (at $\gamma=0$) to $n=2$ (at $\gamma\neq 0$), but the order of precision of the processed splitting propagation grows from $K=2$ (at $\alpha=\beta=\gamma=0$, when it reduces to the genuine Verlet signature) to $K=4$ (at $-\alpha=\beta=\gamma=1/12$).

Because $\mathcal{T}_{\alpha,\beta}^{-1}\mathcal{T}_{\alpha,\beta}=1$, the solution to the equations of motion can now be cast for any t as $\boldsymbol{\rho}(t)=\mathcal{T}_{\alpha,\beta}^{-1}(e^{\tilde{\mathcal{B}}_\gamma h/2}e^{\tilde{\mathcal{A}}h}e^{\tilde{\mathcal{B}}_\gamma h/2})^k\mathcal{T}_{\alpha,\beta}\boldsymbol{\rho}(0)+\mathcal{O}(h^4)$. Then the processing transformation $\mathcal{T}_{\alpha,\beta}$ can be performed only once at the very beginning, and the inverse transformation $\mathcal{T}_{\alpha,\beta}^{-1}$ only once at the end of the considered time interval $[0,t]$. In view of this, the step-by-step integration can be interpreted as the time propagation of pseudovariables $\tilde{\boldsymbol{\rho}}$ by the kernel splitting $e^{\tilde{\mathcal{B}}_\gamma h/2}e^{\tilde{\mathcal{A}}h}e^{\tilde{\mathcal{B}}_\gamma h/2}$ in the transformed phase space. The real phase coordinates $\boldsymbol{\rho}$ are not involved explicitly in the consecutive updating process. They can be reproduced from $\tilde{\boldsymbol{\rho}}$ whenever it is necessary (for example, when measurement is desired) using the inverse transformation $\boldsymbol{\rho}=\mathcal{T}_{\alpha,\beta}^{-1}\tilde{\boldsymbol{\rho}}$. This transformation reads [cf. Eq. (4)]

$$\mathbf{r} = \tilde{\mathbf{r}} - \alpha m^{-1}\mathbf{f}(\tilde{\mathbf{r}},\tilde{\mathbf{S}})h^2, \quad \mathbf{p} = \tilde{\mathbf{p}} - \beta\dot{\mathbf{f}}(\tilde{\boldsymbol{\rho}})h^2,$$

$$\mathbf{S} = \Theta(-\mathbf{J}^{-1}\tilde{\mathbf{S}}\mathbf{g}(\tilde{\mathbf{r}},\tilde{\mathbf{S}}),\alpha h^2)\tilde{\mathbf{S}}, \quad \mathbf{q} = \tilde{\mathbf{q}} - \beta\dot{\mathbf{g}}(\tilde{\boldsymbol{\rho}})h^2, \quad (6)$$

where the higher-order terms $\mathcal{O}(h^4)$ have been neglected since they are not accumulated in $\boldsymbol{\rho}(t)$.

The next crucial point concerns the evaluation of time derivatives $\dot{\mathbf{f}}(\tilde{\boldsymbol{\rho}})$ and $\dot{\mathbf{g}}(\tilde{\boldsymbol{\rho}})$ which arise in Eq. (6). It is obvious that their direct evaluation should be avoided since this results in complicated gradient terms. Fortunately, the derivatives can be evaluated at a given t in a quite efficient way by the symmetric interpolation $\{\dot{\mathbf{f}},\dot{\mathbf{g}}\}(\tilde{\boldsymbol{\rho}})=[\{\tilde{\mathbf{f}},\tilde{\mathbf{g}}\}(t+h)-\{\tilde{\mathbf{f}},\tilde{\mathbf{g}}\}(t-h)]/(2h)+\mathcal{O}(h^2)$, where $\{\tilde{\mathbf{f}},\tilde{\mathbf{g}}\}(t\pm h)=\{\mathbf{f},\mathbf{g}\}(\tilde{\mathbf{r}}(t\pm h),\tilde{\mathbf{S}}(t\pm h))$. Such an interpolation is indeed realizable because the pseudovariables $\tilde{\boldsymbol{\rho}}(t\pm h)$ are determined step by step in the course of the kernel propagation independently of $\boldsymbol{\rho}(t)$. Then the real variables $\boldsymbol{\rho}(t)$ can be reproduced from $\tilde{\boldsymbol{\rho}}(t)$ with a one-step retardation, when the pseudophase coordinates were already propagated to $\tilde{\boldsymbol{\rho}}(t+h)$. This avoids the calculation of extra forces and torques during the interpolation and involves only those that were already evaluated within the kernel propagation. The time derivatives $\dot{\mathbf{f}}(\boldsymbol{\rho})$ and $\dot{\mathbf{g}}(\boldsymbol{\rho})$ in Eq. (4) can be evaluated as $\{\dot{\mathbf{f}},\dot{\mathbf{g}}\}(\boldsymbol{\rho})=[\{\mathbf{f},\mathbf{g}\}(\frac{h}{2})-\{\mathbf{f},\mathbf{g}\}(-\frac{h}{2})]/h+\mathcal{O}(h^2)$, where $\{\mathbf{f},\mathbf{g}\}(\pm\frac{h}{2})=\{\mathbf{f},\mathbf{g}\}(\mathbf{r}(\pm\frac{h}{2}),\mathbf{S}(\pm\frac{h}{2}))$ with $\mathbf{r}(\pm\frac{h}{2})=\mathbf{r}(0)\pm m^{-1}\mathbf{p}(0)\frac{h}{2}$ and $\mathbf{S}(\pm\frac{h}{2})=\Theta(\pm\mathbf{J}^{-1}\mathbf{S}(0)\mathbf{q}(0),\frac{h}{2})\mathbf{S}(0)$. This involves two extra forces and torques at $\pm h/2$ but exclusively at the first step of the integration when starting from an initial configuration $\boldsymbol{\rho}(0)$ and performing the direct transformation $\mathcal{T}_{\alpha,\beta}$.

We see therefore that the processed splitting (PS) algorithm derived is truly of the fourth order and requires only $n=2$ force-torque evaluations per time step. This overcomes the barrier $n=3$ inherent in standard schemes. Moreover, the algorithm is time reversible [because the exponential operators enter symmetrically into the propagator Eq. (3)] and phase-area preserving [since simple shifts and rotations Eq. (5) do not change the volume]. In addition, the algorithm is explicit (no iterations) and exactly conserves the rigid molecular structure (because Ξ and Θ are rotational matrices). The kernel splitting can also be made symplectic, because it is based on a Verlet-like signature which at $\gamma=0$ conserves a nearby Hamiltonian [15,20,21]. For a finite $\gamma \neq 0$, the potential operator can be represented by $\tilde{B}_\gamma = \tilde{B}_0 + \gamma[\tilde{B}_0, [\tilde{A}, \tilde{B}_0]]h^2/2 + \mathcal{O}(h^4)$, where $[\tilde{B}_0, [\tilde{A}, \tilde{B}_0]] = (\tilde{B}_\varepsilon - \tilde{B}_0)/\varepsilon + \mathcal{O}(\varepsilon h^4)$ with $\varepsilon \ll 1$. Then the modified force and torque in \tilde{B}_γ can be evaluated as $\mathbf{f}(\tilde{\mathbf{r}}_\gamma, \tilde{\mathbf{S}}_\gamma) = \mathbf{f}(\tilde{\mathbf{r}}, \tilde{\mathbf{S}}) + \gamma \Delta \mathbf{f}(\tilde{\mathbf{r}}, \tilde{\mathbf{S}})$ and $\mathbf{g}(\tilde{\mathbf{r}}_\gamma, \tilde{\mathbf{S}}_\gamma) = \mathbf{g}(\tilde{\mathbf{r}}, \tilde{\mathbf{S}}) + \gamma \Delta \mathbf{g}(\tilde{\mathbf{r}}, \tilde{\mathbf{S}})$, where the secondary fields are $\Delta \mathbf{f}(\tilde{\mathbf{r}}, \tilde{\mathbf{S}}) = [\mathbf{f}(\tilde{\mathbf{r}}_\varepsilon, \tilde{\mathbf{S}}_\varepsilon) - \mathbf{f}(\tilde{\mathbf{r}}, \tilde{\mathbf{S}})]/\varepsilon + \mathcal{O}(\varepsilon h^4)$ and $\Delta \mathbf{g}(\tilde{\mathbf{r}}, \tilde{\mathbf{S}}) = [\mathbf{g}(\tilde{\mathbf{r}}_\varepsilon, \tilde{\mathbf{S}}_\varepsilon) - \mathbf{g}(\tilde{\mathbf{r}}, \tilde{\mathbf{S}})]/\varepsilon + \mathcal{O}(\varepsilon h^4)$. The parameter ε is typically taken to be of order 10^{-4} for double precision arithmetic to minimize the effect of $\mathcal{O}(\varepsilon h^4)$ terms while avoiding round-off truncations. The processing transformations [Eqs. (4) and (6)] need not be necessarily symplectic, since their effects are not propagated ($\mathcal{T}_{\alpha,\beta}^{-1} \mathcal{T}_{\alpha,\beta} = 1$).

That is very surprising, within the PS method the number n of force-torque recalculations per time step can be reduced to $n=1$ when a quasi-fourth-order calculation is requested. Note that the true fourth order means that the deviations of the generated trajectories $\boldsymbol{\rho}(t)$ from their exact counterparts are equal to $\mathcal{O}(h^4) \sim Ch^4$ at $t \gg h$. In MD simulations, this strong requirement may not be needed, because according to the Lyapunov theorem [3] the coefficient $C \sim e^{\lambda t}$ grows ($\lambda > 0$) exponentially with increasing t . Then the concept of the quasi-fourth-order can be more useful. It implies that the deviations apply not to individual variables of each particle but rather to a collective function for which C is independent of t . In microcanonical simulations such a function should be the total energy $E = \frac{1}{2} \sum_{i=1}^N (\mathbf{p}_i^2/m + \boldsymbol{\Omega}_i \mathbf{J} \boldsymbol{\Omega}_i) + \frac{1}{2} \sum_{i \neq j, a, b} \varphi^{ab}(|\mathbf{r}_i - \mathbf{r}_j|, \mathbf{S}_i, \mathbf{S}_j)$ of the system, where φ^{ab} denotes the intermolecular atom-atom potentials, and M is the number of atoms per molecule. Cumbersome analysis shows that E can be conserved with fourth-order accuracy at $n=1$ by tuning the parameters of the method to $\alpha = -1/24$, $\beta = 1/12$, $\gamma = 0$, and $\eta = 1/48$ [then $\boldsymbol{\rho}(t)$ and other quantities will not be necessarily reproduced up to the fourth order]. Here we should add a new η term when transforming the angular momentum Eq. (6) as

$$\mathbf{q} = \tilde{\mathbf{q}} - \beta \tilde{\mathbf{g}}(\tilde{\boldsymbol{\rho}})h^2 + \eta \tilde{\mathbf{S}}^+ [\mathbf{J} \mathbf{W} (\mathbf{J}^{-1} \tilde{\mathbf{S}} \tilde{\mathbf{q}}) \mathbf{J}^{-1} - \mathbf{W} (\mathbf{J}^{-1} \tilde{\mathbf{S}} \tilde{\mathbf{q}}) - \mathbf{W} (\tilde{\mathbf{S}} \tilde{\mathbf{q}}) \mathbf{J}^{-1}] \tilde{\mathbf{S}} \mathbf{g}(\tilde{\mathbf{r}}, \tilde{\mathbf{S}}) h^2,$$

where $\tilde{\mathbf{S}}^+$ is the transposed matrix [and we correspondingly modify Eq. (4)]. This addition presents no difficulty since $\mathbf{g}(\tilde{\mathbf{r}}, \tilde{\mathbf{S}})$ was already calculated during the kernel splitting. For

systems without periodic boundary conditions, e.g., in celestial mechanics, the total angular momentum is often also conserved. It will be kept with second-order accuracy by the quasi-fourth-order integrator ($n=1$). This is in contrast to the genuine fourth-order algorithm ($n=2$) which produces all quantities to within $\mathcal{O}(h^4)$ precision. Therefore, the former integrator may be less universally applicable than the latter. The PS algorithms will be referred to as PS1 ($n=1$) and PS2 ($n=2$), respectively.

Further improvements are possible by splitting the atom-atom potentials into short- and long-range parts. Then a multiple-time stepping (MTS) technique [22] can be employed, where the expensive long-range (weak) forces are sampled less frequently using larger time steps, while the short-range (strong) interactions are integrated more accurately inside the kernel propagator using smaller steps. The MTS implementation within the PS method goes beyond the scope of this paper and will be considered elsewhere.

III. NUMERICAL RESULTS

We first present the proposed PS method (see Sec. II) in algorithmic form to simplify its numerical implementation. Thus, starting at $t=0$ from an initial configuration $\boldsymbol{\rho}(0) = \{\mathbf{r}(0), \mathbf{p}(0), \mathbf{S}(0), \mathbf{q}(0)\}$ and calculating the three forces $\mathbf{f}(0)$ and $\mathbf{f}(\pm h/2)$ as well as the three torques $\mathbf{g}(0)$ and $\mathbf{g}(\pm h/2)$ at the positions $\{\mathbf{r}(0), \mathbf{S}(0)\}$ and $\{\mathbf{r}(\pm h/2), \mathbf{S}(\pm h/2)\}$, respectively, where $\mathbf{r}(\pm h/2) = \mathbf{r}(0) \pm m^{-1} \mathbf{p}(0) h/2$ and $\mathbf{S}(\pm h/2) = \Theta(\pm \mathbf{J}^{-1} \mathbf{S}(0) \mathbf{q}(0), h/2) \mathbf{S}(0)$, we make the direct processing transformation [Eq. (4)] to $\tilde{\boldsymbol{\rho}}(0) = \{\tilde{\mathbf{r}}(0), \tilde{\mathbf{p}}(0), \tilde{\mathbf{S}}(0), \tilde{\mathbf{q}}(0)\}$ as

$$\begin{aligned} \tilde{\mathbf{r}}(0) &= \mathbf{r}(0) + \alpha m^{-1} \mathbf{f}(0) h^2, \\ \tilde{\mathbf{S}}(0) &= \Theta(\mathbf{J}^{-1} \mathbf{S}(0) \mathbf{g}(0), \alpha h^2) \mathbf{S}(0), \\ \tilde{\mathbf{p}}(0) &= \mathbf{p}(0) + \beta (\mathbf{f}(h/2) - \mathbf{f}(-h/2)) h, \\ \tilde{\mathbf{q}}(0) &= \mathbf{q}(0) + \beta (\mathbf{g}(h/2) - \mathbf{g}(-h/2)) h. \end{aligned} \quad (7)$$

Having $\tilde{\boldsymbol{\rho}}(0)$, we calculate the two initial forces $\tilde{\mathbf{f}}(0)$ and $\tilde{\mathbf{f}}_\varepsilon(0)$ as well as the two initial torques $\tilde{\mathbf{g}}(0)$ and $\tilde{\mathbf{g}}_\varepsilon(0)$ at the positions $\{\tilde{\mathbf{r}}(0), \tilde{\mathbf{S}}(0)\}$ and $\{\tilde{\mathbf{r}}_\varepsilon(0), \tilde{\mathbf{S}}_\varepsilon(0)\}$, respectively, where $\tilde{\mathbf{r}}_\varepsilon(0) = \tilde{\mathbf{r}}(0) + \varepsilon m^{-1} \tilde{\mathbf{f}}(0) h^2$ and $\tilde{\mathbf{S}}_\varepsilon(0) = \Theta(\mathbf{J}^{-1} \tilde{\mathbf{S}}(0) \tilde{\mathbf{g}}(0), \varepsilon h^2) \tilde{\mathbf{S}}(0)$. Note that the direct transformation Eq. (7) as well as the evaluation of the initial forces and torques should be carried out only once at the very beginning ($t=0$) of the integration.

Now we perform the single-step propagations of $\tilde{\boldsymbol{\rho}}$ from time t to $t+h$ according to the kernel splitting Eq. (3) as

$$\tilde{\mathbf{p}}_{t+h/2} = \tilde{\mathbf{p}}(t) + \left(\tilde{\mathbf{f}}(t) + \frac{\gamma}{\varepsilon} [\tilde{\mathbf{f}}_\varepsilon(t) - \tilde{\mathbf{f}}(t)] \right) \frac{h}{2},$$

$$\tilde{\mathbf{q}}_{t+h/2} = \tilde{\mathbf{q}}(t) + \left(\tilde{\mathbf{g}}(t) + \frac{\gamma}{\varepsilon} [\tilde{\mathbf{g}}_\varepsilon(t) - \tilde{\mathbf{g}}(t)] \right) \frac{h}{2},$$

$$\tilde{\mathbf{r}}(t+h) = \tilde{\mathbf{r}}(t) + m^{-1} \tilde{\mathbf{p}}_{t+h/2} h,$$

$$\begin{aligned}\tilde{\mathbf{S}}(t+h) &= \Xi(\tilde{\mathbf{q}}_{t+h/2}, h)\tilde{\mathbf{S}}(t), \\ \tilde{\mathbf{p}}(t+h) &= \tilde{\mathbf{p}}_{t+h/2} + \left(\tilde{\mathbf{f}}(t+h) + \frac{\gamma}{\varepsilon}[\tilde{\mathbf{f}}_{\varepsilon}(t+h) - \tilde{\mathbf{f}}(t+h)] \right) \frac{h}{2}, \\ \tilde{\mathbf{q}}(t+h) &= \tilde{\mathbf{q}}_{t+h/2} + \left(\tilde{\mathbf{g}}(t+h) + \frac{\gamma}{\varepsilon}[\tilde{\mathbf{g}}_{\varepsilon}(t+h) - \tilde{\mathbf{g}}(t+h)] \right) \frac{h}{2},\end{aligned}\quad (8)$$

where $\tilde{\mathbf{p}}_{t+h/2}$ and $\tilde{\mathbf{q}}_{t+h/2}$ are the intermediate values, and the two new forces $\tilde{\mathbf{f}}(t+h)$ and $\tilde{\mathbf{f}}_{\varepsilon}(t+h)$ as well as the two new torques $\tilde{\mathbf{g}}(t+h)$ and $\tilde{\mathbf{g}}_{\varepsilon}(t+h)$ should be calculated at the new positions $\{\tilde{\mathbf{r}}(t+h), \tilde{\mathbf{S}}(t+h)\}$ and $\{\tilde{\mathbf{r}}_{\varepsilon}(t+h), \tilde{\mathbf{S}}_{\varepsilon}(t+h)\}$, respectively, with $\tilde{\mathbf{r}}_{\varepsilon}(t+h) = \tilde{\mathbf{r}}(t+h) + \varepsilon m^{-1} \tilde{\mathbf{f}}(t+h) h^2$ and $\tilde{\mathbf{S}}_{\varepsilon}(t+h) = \Theta(\mathbf{J}^{-1} \tilde{\mathbf{S}}(t+h) \tilde{\mathbf{g}}(t+h), \varepsilon h^2) \tilde{\mathbf{S}}(t+h)$ before the evaluation of $\tilde{\mathbf{p}}(t+h)$ and $\tilde{\mathbf{q}}(t+h)$. Saving the forces $\tilde{\mathbf{f}}(t+h)$ and $\tilde{\mathbf{f}}_{\varepsilon}(t+h)$ as well as the torques $\tilde{\mathbf{g}}(t+h)$ and $\tilde{\mathbf{g}}_{\varepsilon}(t+h)$, we repeat Eq. (8) (with formal replacement of t by $t+h$) to propagate $\tilde{\mathbf{p}}$ from time $t+h$ to $t+2h$. In this way, step by step we can recycle Eq. (8) an arbitrary number $k \geq 1$ of times and obtain the value of $\tilde{\mathbf{p}}(t)$ for any $t = kh$. Each recycle will require the recalculation of only two ($n=2$) new forces and torques.

When at least two recycles of Eq. (8) have been done already, we will have the three consecutive values $\tilde{\mathbf{p}}(t-h)$, $\tilde{\mathbf{p}}(t)$, and $\tilde{\mathbf{p}}(t+h)$ for some $t = kh$. The forces $\tilde{\mathbf{f}}(t)$ and $\tilde{\mathbf{f}}(t \pm h)$ as well as the torques $\tilde{\mathbf{g}}(t)$ and $\tilde{\mathbf{g}}(t \pm h)$ will also be already known because of the kernel propagations. Then we can make the inverse processing transformation Eq. (6) of $\tilde{\mathbf{p}}(t)$ to the genuine value $\mathbf{p}(t)$ at a current t according to

$$\begin{aligned}\mathbf{r}(t) &= \tilde{\mathbf{r}}(t) - \alpha m^{-1} \tilde{\mathbf{f}}(t) h^2, \\ \mathbf{S}(t) &= \Theta(-\mathbf{J}^{-1} \tilde{\mathbf{S}}(t) \tilde{\mathbf{g}}(t), \alpha h^2) \tilde{\mathbf{S}}(t), \\ \mathbf{p}(t) &= \tilde{\mathbf{p}}(t) - \beta(\tilde{\mathbf{f}}(t+h) - \tilde{\mathbf{f}}(t-h)) h/2, \\ \mathbf{q}(t) &= \tilde{\mathbf{q}}(t) - \beta(\tilde{\mathbf{g}}(t+h) - \tilde{\mathbf{g}}(t-h)) h/2,\end{aligned}\quad (9)$$

and calculate at this point all necessary observable quantities (such as the total energy, etc.). This completes the PS2 algorithm ($n=2$), where $\alpha = -1/12$, $\beta = 1/12$, and $\gamma = 1/12$. The PS1 integrator ($n=1$) follows at $\alpha = -1/24$, $\beta = 1/12$, $\gamma = 0$, and $\eta = 1/48$ [here the evaluation of the modified force $\tilde{\mathbf{f}}_{\varepsilon}$ and torque $\tilde{\mathbf{g}}_{\varepsilon}$ should be omitted in Eq. (8) since $\gamma = 0$, while the inclusion of the η term in Eqs. (7) and (9) is trivial].

For testing of the algorithms we applied the transferable interaction potential with four points (TIP4P) model ($M=4$) of water [23] with $N=512$ molecules. The MD simulations were carried in the microcanonical (NVE) ensemble at a density of $N/V=1$ g/cm³ and a temperature of 292 K. The Ewald summation [24] was exploited to handle long-range Coulombic atom interactions. The accuracy of the simulations was measured by calculating the ratio \mathcal{R} of the fluctuations of the total energy E to the fluctuations of its potential part [15]. The computational costs Y were estimated in terms of the number of force-torque evaluations in a given time

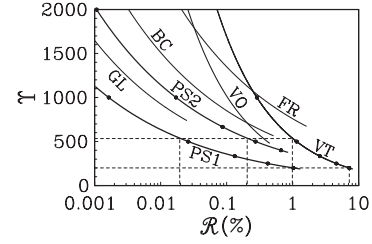


FIG. 1. Cost versus relative error for different algorithms in MD simulations of water. The circles correspond to the time steps (left to right) $h=1, 2, 3, 4,$ and 5 fs. The dashed lines represent the most characteristic levels.

interval, taken to be $\Lambda=1$ ps, so that $Y=n\Lambda/h$. The equations of motion were solved at several sizes of the time step ranging from $h=0.5$ to 5 fs. In total, $k=t/h=10^5$ steps were used for each algorithm and each step size.

The costs Y versus precision \mathcal{R} of the integration obtained within the two proposed PS algorithms ($K=4$) at the end of the simulations are plotted in Fig. 1 by the curves marked as PS1 ($n=1$) and PS2 ($n=2$), respectively. The results corresponding to the Verlet-type (VT) algorithm ($K=2$ and $n=1$), its optimized (VO) version ($K=2$ and $n=2$), the Forest-Ruth (FR) scheme ($K=4$ and $n=3$), as well as the gradientlike (GL) algorithm ($K=4$ and $n=3$) (these integrators are described in Refs. [15,21]) were also included for the purpose of comparison. It has been established that other known rigid-body integrators [8–12,25] ($K=2$ and $n=1$) behave similarly to the VT algorithm. Higher-order schemes [15,26] with $K \geq 4$ and $n \geq 4$ are less efficient in MD simulations because of the large numbers of costly force-torque recalculations. The processed fourth-order algorithm by Blanes and Casas (BC) *et al.* [16,19] with $K=4$ and $n=1 + \nu=3$ [where the kernel and processor are defined according to Eqs. (20) and (21) of Ref. [16]] was adapted to rigid-body motion and considered too.

As can be seen from Fig. 1, with decreasing Y (increasing h) each curve terminates at some point where the simulations begin to exhibit a drift in \mathcal{R} . This happens around $h \sim 5$ fs (larger h can be used within the MTS). At the minimal possible cost $Y \sim 200$, the VT integrator can provide only a crude energy conservation $\mathcal{R} \sim 7\%$. This level of errors is too large and generally unacceptable in MD simulations. It should be reduced at least to $\mathcal{R} \sim 1\%$, arguably the upper limit of allowable error for which the dynamics can be simulated adequately. The proposed PS1 algorithm just satisfies this criterion even at $Y \sim 200$. On the other hand, the level $\mathcal{R} \sim 1\%$ can be achieved by the VT integrator by increasing the load to $Y \sim 550$, i.e., by a factor of 2.75. Thus the PS1 algorithm may use considerably smaller CPU time at a given precision. The PS2 algorithm is also superior to the VT scheme. For more accurate ($\mathcal{R} < 1\%$) simulations, the relative efficiency of the PS algorithms ($K=4$) with respect to the VT scheme ($K=2$) rises further (because $\mathcal{R} \sim h^K$) and reaches a factor of 5 at $\mathcal{R} \sim 0.1\%$. At the same time, for $Y \sim 550$ the PS2 and PS1 algorithms are able to lower the numerical errors from the value $\mathcal{R} \sim 1\%$ inherent in the VT integrator to the levels $\mathcal{R} \sim 0.2\%$ and 0.02% , respectively, i.e., up to 50 times. The VO integrator is clearly inferior to

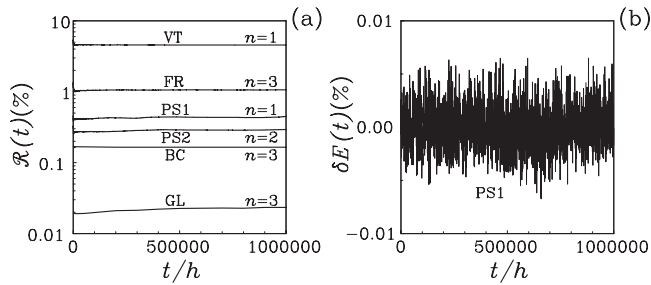


FIG. 2. Fluctuations (a) and deviations (b) of the total energy versus the length of the MD simulations carried out at $h=4$ fs using different algorithms.

the PS algorithms, although it is better than the VT signature. The BC scheme can be superior to the VO integrator but worse than the PS algorithms. The FR scheme leads to the worst efficiency. The GL algorithm can be used only at $Y > 750$, i.e., when a very high accuracy ($\mathcal{R} \leq 0.02\%$) is required. Then it appears to be more efficient than the PS2 integrator. However, the PS1 algorithm is the best in the whole Y region.

Samples of the relative fluctuations $\mathcal{R}(t)$ and normalized deviations $\delta E(t) = [E(t) - E(0)]/E(0)$ of the instantaneous total energy $E(t)$ are shown in Figs. 2(a) and 2(b), respectively, versus the length t/h of the simulations performed at a typical step $h=4$ fs using different integrators. We can observe in Fig. 2(a) that the functions $\mathcal{R}(t)$ are flat with no drift in the entire time domain. The PS algorithms, apart from their high

efficiency, also exhibit excellent stability properties. As is illustrated in Fig. 2(b) for the PS1 method, the total energy $E(t)$ continues to remain near its initial value $E(0)$ even after an extremely long period of time with $k=10^6$ steps. The magnitude of the deviations $\delta E(t)$ is quite small and does not exceed a level of 0.01%, making the energy conservation almost exact.

IV. CONCLUSION

In this paper we have proposed a method for the integration of motion in rigid-body MD simulations that combines standard splitting techniques with special phase-space processing transformations. Comparison with well-recognized previous schemes has demonstrated that our method allows us to significantly improve the efficiency of the integration with no extra computational costs. The algorithms obtained are easy in implementation and can readily be incorporated into existing MD codes. They can also be applied to hybrid Monte Carlo and MD simulations of simple fluids and to other fields mentioned in the Introduction as well as being extended to more complicated systems with flexible molecules.

ACKNOWLEDGMENT

The author acknowledges support by the Fonds zur Förderung der Wissenschaftlichen Forschung under the Project No. P18592-TPH.

-
- [1] M. P. Allen and D. J. Tildesley, *Computer Simulation of Liquids* (Clarendon, Oxford, 1987).
- [2] D. C. Rapaport, *The Art of Molecular Dynamics Simulation* (Cambridge University Press, Cambridge, U.K., 1995).
- [3] D. Frenkel and B. Smit, *Understanding Molecular Simulation: from Algorithms to Applications* (Academic Press, New York, 1996).
- [4] S. Essiz and R. D. Coalson, *J. Chem. Phys.* **124**, 144116 (2006).
- [5] E. Celledoni and N. Säfström, *J. Phys. A* **39**, 5463 (2006).
- [6] S. A. Chin, *Phys. Rev. E* **75**, 036701 (2007).
- [7] S. Reich, *Fields Inst. Commun.* **10**, 181 (1996).
- [8] A. Kol, B. B. Laird, and B. J. Leimkuhler, *J. Chem. Phys.* **107**, 2580 (1997).
- [9] A. Dullweber, B. Leimkuhler, and R. McLachlan, *J. Chem. Phys.* **107**, 5840 (1997).
- [10] N. Matubayasi and M. Nakahara, *J. Chem. Phys.* **110**, 3291 (1999).
- [11] T. F. Miller III, M. Eleftheriou, P. Pattnaik, A. Ndirango, D. Newns, and G. J. Martyna, *J. Chem. Phys.* **116**, 8649 (2002).
- [12] H. Kamberaj, R. J. Low, and M. P. Neal, *J. Chem. Phys.* **122**, 224114 (2005).
- [13] I. P. Omelyan, I. M. Mryglod, and R. Folk, *Comput. Phys. Commun.* **151**, 272 (2003).
- [14] I. P. Omelyan, *Phys. Rev. E* **74**, 036703 (2006).
- [15] I. P. Omelyan, *J. Chem. Phys.* **127**, 044102 (2007).
- [16] S. Blanes, F. Casas, and J. Ros, *SIAM J. Sci. Comput. (USA)* **21**, 711 (1999).
- [17] R. D. Skeel, G. Zhang, and T. Schlick, *SIAM J. Sci. Comput. (USA)* **18**, 203 (1997).
- [18] M. A. López-Marcos, J. M. Sanz-Serna, and R. D. Skeel, *SIAM J. Sci. Comput. (USA)* **18**, 223 (1997).
- [19] S. Blanes, F. Casas, and A. Murua, *SIAM J. Sci. Comput. (USA)* **42**, 531 (2004); **27**, 1817 (2006).
- [20] R. van Zon and J. Schofield, *Phys. Rev. E* **75**, 056701 (2007).
- [21] R. van Zon, I. P. Omelyan, and J. Schofield, *J. Chem. Phys.* **128**, 136102 (2008).
- [22] M. E. Tuckerman, B. J. Berne, and G. J. Martyna, *J. Chem. Phys.* **97**, 1990 (1992).
- [23] W. L. Jorgensen, J. Chandrasekhar, J. D. Madura, R. W. Impey, and M. L. Klein, *J. Chem. Phys.* **79**, 926 (1983).
- [24] I. P. Omelyan, *Comput. Phys. Commun.* **107**, 113 (1997).
- [25] J. P. Ryckaert, G. Ciccotti, and H. J. C. Berendsen, *J. Comput. Phys.* **23**, 327 (1977).
- [26] S. Blanes and F. Casas, *J. Phys. A* **39**, 5405 (2006).